JOURNAL OF MATERIALS SCIENCE **38** (2003) 3169–3181

Process intensification in particle technology: Intensive granulation mechanism and granule characteristics

G. AKAY*, L. TONG
Process Intensification and Miniaturisation Centre, School of Chemical Engineering and Advanced Materials, University of Newcastle, Newcastle upon Tyne NE1 7RU, UK
E-mail: galip.akay@newcastle.ac.uk

The mechanism and processing characteristics of a novel intensified granulation technique are evaluated. This intensification technique is based on the non-isothermal flow induced phase inversion (FIPI) phenomenon. Poly(ethylene glycol) (PEG) with an average molecular weight 10^4 and calcium carbonate powder (mean particle size 2.7 μm) were used as binder and filler to prepare granules. The granulation experiments were carried using a Haake extruder (Rheomex 252) which connected to a granulator of a new design. The extruder produced a homogenous PEG and calcium carbonate paste and fed it to the granulator. When the paste was subjected to a temperature gradient field with a superimposed repeated shear and extensional deformation, solidification, granule nucleation and subsequent macroscopic fragmentation (referred to as crumbling) occurred to give granular particles. The mechanism of granulation has been discussed. The granule size and size distribution characteristics under different process conditions have been evaluated. The novelty of this research lies in the granulator design and the mechanism of the granulation process. Temperature differential and repeated deformation are the two primary factors for the granulation process. Particle size distribution and crumbling area depend on the concentration of PEG, the clearance between rotor and stator, and the extrusion speed. If a so called 'crumbling agent', in the form of fine particles, is added to the newly formed granules, these granules are coated with the crumbling agent forming a core-shell type of granulated particles.

List of symbols

C_P	Concentration of polymer (PEG molecular weight 10^4) in the melt (wt%)
C_F	Concentration of calcium carbonate in the melt (wt%)
G_U	Upper rotor/stator clearance (mm)
G_L	Lower rotor/stator clearance (mm)
ΔH_c	Heat of crystallisation
ΔH_m	Heat of melting
Ω_E	Extruder screw speed (rpm)
Ω_R	Rotor speed (rpm)

Particle size characterisation

$D(10)$, $D(50)$, $D(90)$	Granule diameters below which 10, 50, 90% of the particles lie respectively.
$D(50)$	Primary particle diameter below which 50% of the particles lie.
S	Particle size span ($S = [D(90) - D(10)]/D(50)$)

Temperatures used in characterisation by DSC

$T_c(10\%)$	Crystallisation onset temperature (10% solidifies) (°C)
$T_c(95\%)$	Crystallisation completion temperature (95% solidifies) (°C)
$T_m(10\%)$	Melting onset temperature (10% melts) (°C)
$T_m(95\%)$	Melting completion temperature (95% melts) (°C)
T_{cp}	Peak crystallisation temperature (°C)
T_{mp}	Peak melting temperature (°C)

Temperatures used in process characterisation

T_E	Extruder exit temperature (°C)
T_{LS}	Set temperature of the lower stator (°C)
T_{LR}	Set temperature of the lower rotor (°C)
T_{US}	Set temperature of the upper stator (°C)
T_{UR}	Set temperature of the upper rotor (°C)

*Author to whom all correspondence should be addressed.

1. Introduction

Granulation is an important process in powder technology whereby small particles are agglomerated or encapsulated in order to achieve safe handling and controlled release of the active materials. Agglomeration and encapsulation of fine particles normally are demanded in pharmaceuticals, detergents, fertilizers, food and coating industrial sectors. The so-called multi-nucleus type capsules/microcapsules are essentially agglomerated particles with prescribed released characteristics which can be controlled by the concentration and solubility of the binder. In agglomeration, the amount of binder is kept to a minimum as long as the agglomerates are sufficiently strong against attrition. Therefore, in principle, multi-nucleus microcapsules can be manufactured through an agglomeration process. Furthermore, a shell-and-core type of microcapsules can be obtained by forming a suitable film around the multi-nucleus microcapsules. Powder granulation includes a number of techniques, particularly by tumbling, agitating, or fluidizing raw materials in the presence of liquid binders to obtain a wide distribution in granule size. If material is forced to flow through dies or a screen followed by cooling to obtain granules, they are called machine-made granules [1–4]. These methods also are classed in terms of binder granulation.

A novel agglomeration technique was developed by Akay [5–9]. This technique is based on the flow induced phase inversion (FIPI) phenomenon [9–11] and was utilized in the agglomeration of fine powders and micro-encapsulation of solids/or liquids as well as emulsification of high viscosity oils or polymer melts in water [9–16]. In FIPI agglomeration and micro-encapsulation, a concentrated suspension of powder in liquid is caused to crumble (phase invert) through the further addition of a powder (a "crumbling agent"), i.e., a phase inversion from a solid phase suspended in liquid (a paste) to a liquid phase suspended in solid (an agglomerated granular material). The process requires a degree of mechanical energy input in order to disperse the two phases and therefore, it must be carried out in some kind of mixing environment. Also, the critical deformation rate at which FIPI starts is dependent on the thermodynamic state of the structured fluid as well as the type of flow field, i.e., shear or extensional or combined flows [9–11, 17]. In certain applications, it is necessary that the flow field should be uniform and the deformation rate should be very high [5–12]. The mixing requirement for FIPI is much less restrictive than it would be in conventional agglomeration since shear can be transmitted to a paste much more effectively than to an agglomerated powder. This mixing flexibility allows FIPI in either a batch or a continuous mode of operation. The FIPI granulation technique combines both growth and pressure agglomeration processes. For a typical isothermal FIPI agglomeration/micro-encapsulation process, the phase inversion takes place at a critical dispersed phase concentration (crumbling concentration) when the primary particle size and mixing conditions are kept constant. This crumbling concentration is as important as the shear flow.

After the initial disclosure of the granulation technique, based on non-isothermal FIPI [11], this phenomenon and its applications have not been studied in any detail. Akay *et al.* [13–16] have shown that in the presence of phase transformation (i.e., from melt to solid), flow (deformation) can also induce phase inversion in water/polymer/polymeric surfactant systems under non-isothermal conditions. The use of temperature and deformation as processing parameters can therefore promote phase inversion in solid particle/polymer systems and can be utilised in process intensification in particle technology. This process is particularly striking if the polymer is crystallisable or has linear molecular chain with high molecular weight since such molecules readily undergo mechano-chemical reactions [17–21] which result in macromolecular deposition on the filler particles [18–21]. In this case, reduction in temperature in polymer melt/particle mixture (paste) results in a reduction of the continuous phase volume due to the crystallisation and stress induced deposition of the higher molecular weight fractions of the polymer. Furthermore, at lower temperature, due to the reduced polymer chain mobility and interactions with the large numbers of small primary particles, which make a 3D cage [5, 8], the effective mobile phase volume decreases further with increasing primary particle concentration. Consequently, the continuous phase can no longer sustain the increased phase volume of the dispersed phase and phase inversion takes place in the form of the melt fracture [6, 9, 13]. This phenomenon now forms the basis of the present granulation technique. The generic granulation techniques described previously are illustrated diagrammatically in Fig. 1.

In the present study, a newly designed and recently built granulator was employed to evaluate the characteristics of the granules and the mechanism of this non-isothermal FIPI intensive granulation technique which can also be termed as 'intensive structuring' [6, 22, 23] due to the formation of micro-structured materials. The operating characteristics of this novel granulator were explored. The mechanism of the intensified granulation process has been investigated. The relationship between granule property and process was studied.

2. Experimental

2.1. Materials

Filler: Calcium carbonate ($CaCO_3$) particles (coded Millicarb-OG) with mean particle size d (50%) about 2.7 μm was supplied by Omya UK Ltd.

Binder: Poly(ethylene glycol) (PEG) with average molecular weight of 10^4 was supplied by Fluka Chemie GmbH. It is in a solid flake form at room temperature. Differential Scanning Calorimetry (DSC) in previous studies [12] have determined the thermal properties of PEG, and the summary of the results is tabulated in Table I for heating and cooling cycles.

2.2. Equipment

The complete granulation process is carried out in a system which is illustrated diagrammatically in Fig. 2.

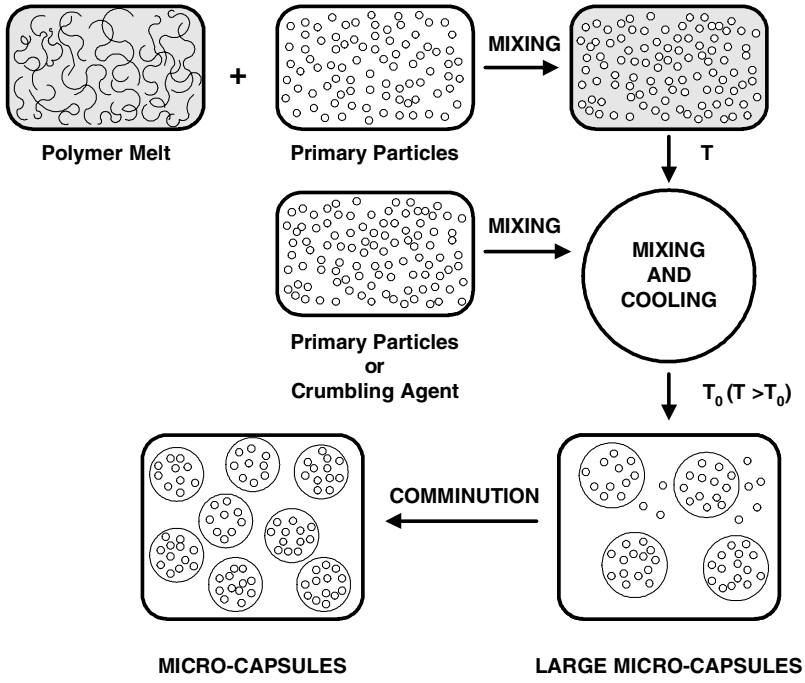

Figure 1 Intensive agglomeration and micro-encapsulation by flow induced phase inversion.

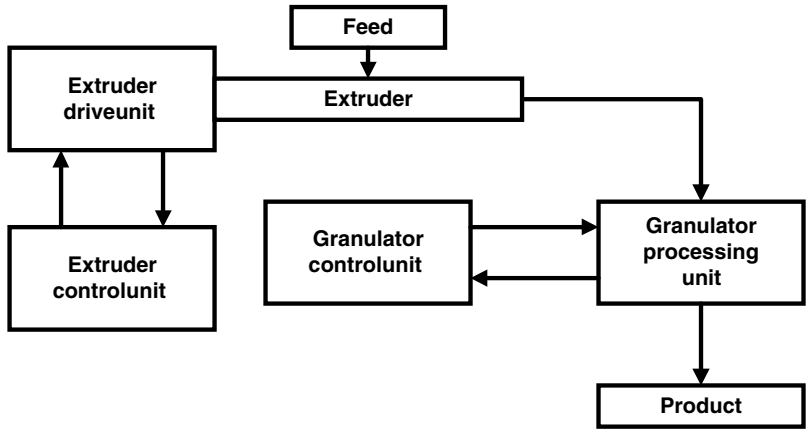

Figure 2 Diagrammatic representation of the processing equipment including extruder, extruder drive unit, extruder control unit, and intensive agglomerator/mocroencapsulator processing and control units.

This system consists of an extruder and granulator processors with their own separate control and data acquisition and display units.

(a) Extruder: Haake extruder, Rheomex 252 was employed in this study. It is a single mixing screw extruder and driven and controlled by the Haake High Torque Rheometer (RC90/9000). In the Rheometer drive unit there is a horizontally mounted heavy duty motor with a torque sensor attached to the extruder screw. The extruder barrel has three temperature control zones. They are controlled by air cooling. The screw torque, speed, pressure at the extruder outlet and temperatures along the barrel can be recorded continuously as a function of time. The extruder was used for melting and mixing the materials and feeding them to the granulator.

(b) Granulator: The granulator is connected to the extruder outlet through a feeding pipe. Fig. 3 is a schematic diagram of the granulator. It consists of two back-to-back rotors (referred to as upper and lower rotors) made from a single circular block and two stators (also referred to as upper and lower stators) facing the rotors. The rotor block is driven by a motor with variable speeds (0–5 rpm or 0–500 rpm) via a gear box. The rotors and stators contain cavities on their surfaces which are designed to pump/convey and/or achieve mixing. These cavities are offset by half a cavity length so that the rotor and stator cavities never exactly match to each other. The separation of the upper (G_U) and lower (G_L) rotor and stator can be varied independently.

On the upper stator there are two melt inlet ports 1 and 2. One is located on the top centre and the other one is on the side of the upper stator. The polymer mixture can be fed in through either port. The polymer melt then flows into the gap between the upper stator and rotor. The gap between the upper and lower rotors and stators can be adjusted by the rotor height adjustment screw or the spacer ring. The rotor block (incorporating the upper and lower rotors) spins sandwiched between the upper stator and lower stator of the granulator. Granulation takes place inside the gap between the upper stator and rotor. Once the granules are formed they travel through

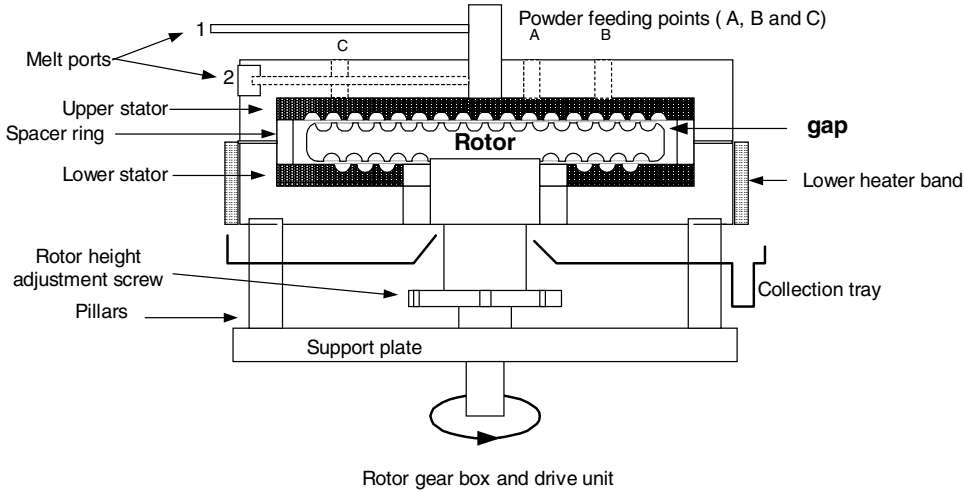

Figure 3 Schematic diagram of the granulator, polymer blend can be fed through ports 1 or 2. The gap between upper stator and rotor can be adjusted by spacer ring or rotor height adjustment screw.

the gap between the lower stator and rotor and finally emerge and drop on to the collection tray.

The upper stator also contains 3 auger powder feeders located symmetrically at various distances from the centre. Additional powder can be added into the filled polymer melt after phase inversion. The addition of the extra powder is useful to increase the particle content of the agglomerates and in forming a shell-and-core type of microcapsules. There are pressure transducers sited at several locations on the upper stator in order to determine the location of the polymer melt and agglomerates. Temperatures of the upper and lower stators are controlled independently. Temperatures of the rotors are kept below that of the corresponding stator temperatures. A more detailed introduction to the granulator can be found in a previous paper [12].

2.3. Experimental procedure

Poly(ethylene glycol) flakes (binder) were blended with calcium carbonate powders (filler) at a desired concentration (C_P = concentration of polymer and C_F = concentration of the filler, in wt%) and fed into the extruder. As shown in Table I [12], the melting temperature range of PEG is from 58 to 66°C during heating cycle. Therefore, the temperature along the extruder barrel (3 zones) was kept constant at $T_E = 70$°C. The extruder screw speed was either $\Omega_E = 10$ rpm or 15 rpm. The polymer/calcium carbonate blend was conveyed along the extruder barrel when the polymer was melted and mixed with the filler and then transferred to the granulator via a heated pipe which formed the connection between the extruder and the centre on the upper stator. Since the results in Table I indicate that the crystallization range of PEG is from 53 to 43°C during the cooling cycle, so the temperature setting of the upper stator (T_{US}) in the experiment was chosen to be 52°C. The temperatures of rotor (T_{UR}) and lower stator (T_{LS}) were set at 45°C. The rotor speed was kept at $\Omega_R = 30$ rpm. The rotational speed needs increasing if the polymer melt is frozen rapidly in the granulation process unit thus causing the blockage of the extruder. If a blockage happens, the extruder torque increases rapidly and in response, the rotor speed is increased to 40 rpm until the blockage is cleared and the speed is restored back to 30 rpm. The temperature profile in the extruder and granulator is dictated by the melting and crystallization characteristics of the binder polymer and polymer and filler mixture.

At the end of each experiment, the extruder and the granulator were stopped and allowed to cool down to the ambient temperature and the upper stator was separated from the rotor. In order to understand the mechanism of granulation and the location of the transition from paste to granules, it is convenient to base the characterization of the granulator through the upper rotor cavity location. The upper stator and rotor were photographed in order to determine the location of the phase inversion and to determine the nature of the structure change during phase transformation

TABLE I DSC results of the PEG and $CaCO_3$ blends at different concentrations

	Heating				Cooling			
		Melting range				Solidification range		
Sample	Melt peak T_{mp} (°C)	T_m (10%) (°C)	T_m (95%) (°C)	ΔH_m (J/g)	Solidification peak T_{cp} (°C)	T_c (10%) (°C)	T_c (95%) (°C)	ΔH_c (J/g)
100.0% PEG	63.2	59.4	65	−171	51.8	52.9	50.3	93
32.5% PEG	63.3	58.8	65.5	−56.3	47.6	49.4	45	36
30.0% PEG	63.1	58.5	65.5	−51.9	46.2	48.9	44.1	30
27.5% PEG	63.3	58.8	66	−48.1	46	48.7	43.4	34.2
25.0% PEG	63.3	58.6	66	−48.9	46	48.4	43.3	32.1

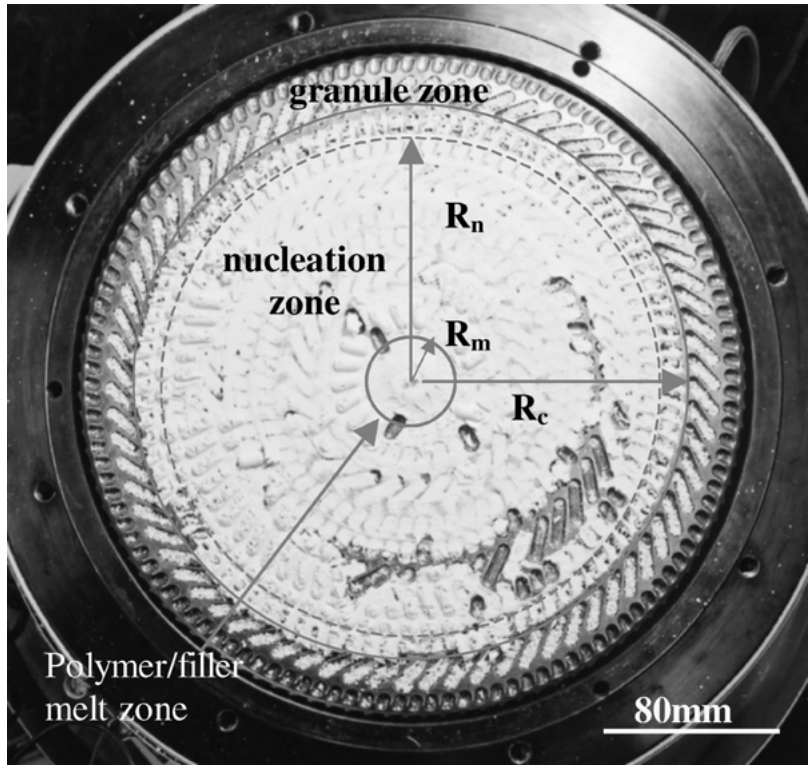

(a)

(b)

Figure 4 Evaluation of the granulation process by visualisation (a) General view of the upper rotor and identification of various zones and their relative size. R_m = radius of the polymer/filler melt zone, R_n = nucleation zone radius, R_c = crumbling zone radius. (b) Enlarged view of the polymer melt/filler melt zone and start of the nucleation zone. (c) View of the upper stator showing the sheared region and cavity region where mixing and nucleation takes place. (d) Corresponding region on the upper rotor in the nucleation zone. (e) Nucleation, crumbling and granule zones on the upper rotor. (f) Corresponding nucleation and crumbling zones on the upper stator which does not contain any granules except those just about to fracture from the bulk. (g) Scanning electron micrograph of the sample recovered from the upper rotor cavity in the nucleation zone showing the presence of micro-mixing and nucleation. (h) Scanning electron micrograph of the sheared region in the nucleation zone on the upper rotor. (i) Scanning electron micrograph of the sample recovered from the region when filled polymer melt expands into the upper rotor after being sheared. This micrograph shows the presence of slow instability. Granules contained 30% PEG and the processing condition were: Melt entry temperature $T_E = 70°C$, upper stator temperature $T_{US} = 52°C$, upper rotor temperature $T_{UR} = 45°C$, lower rotor temperature $T_{LR} = 45°C$ and lower stator temperature $T_{LS} = 45°C$. Upper rotor/stator clearance $G_U = 0.5$ mm and lower rotor/stator clearance $G_L = 0.5$ mm, screw speed $\Omega_E = 10$ rpm, rotor speed $\Omega_R = 30$–40 rpm. (*Continued*)

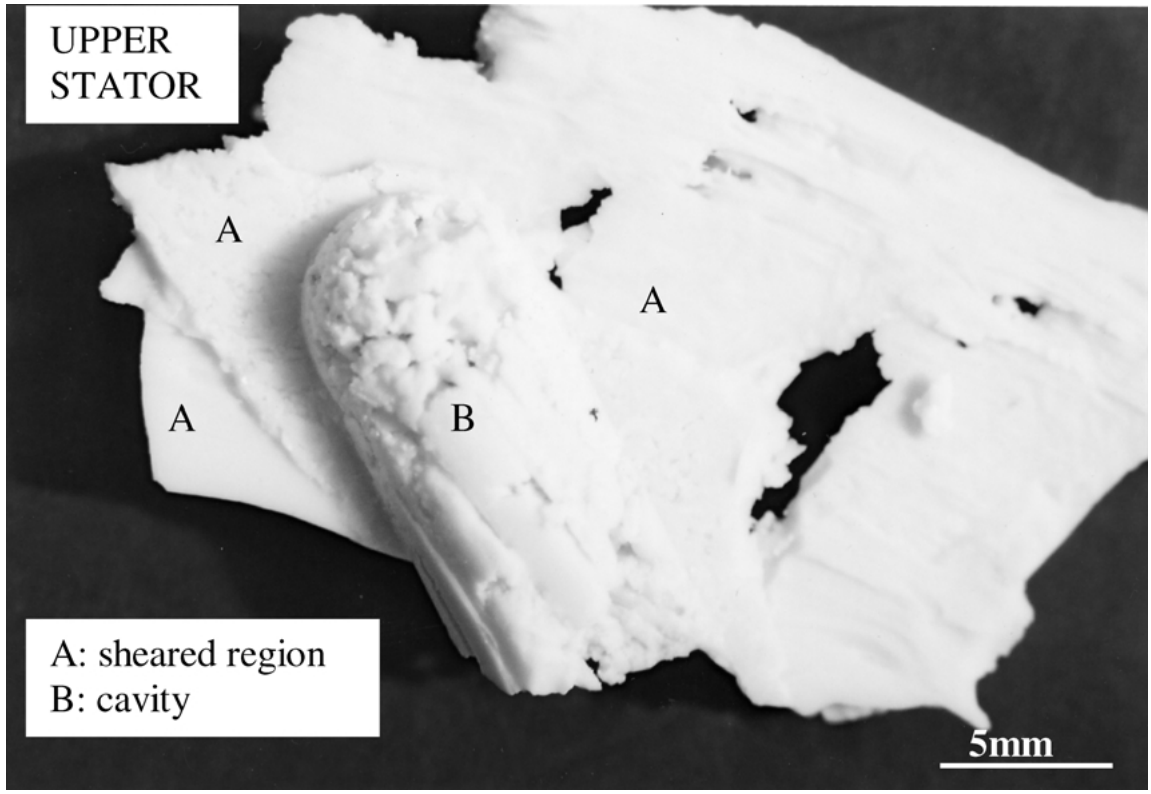

(c)

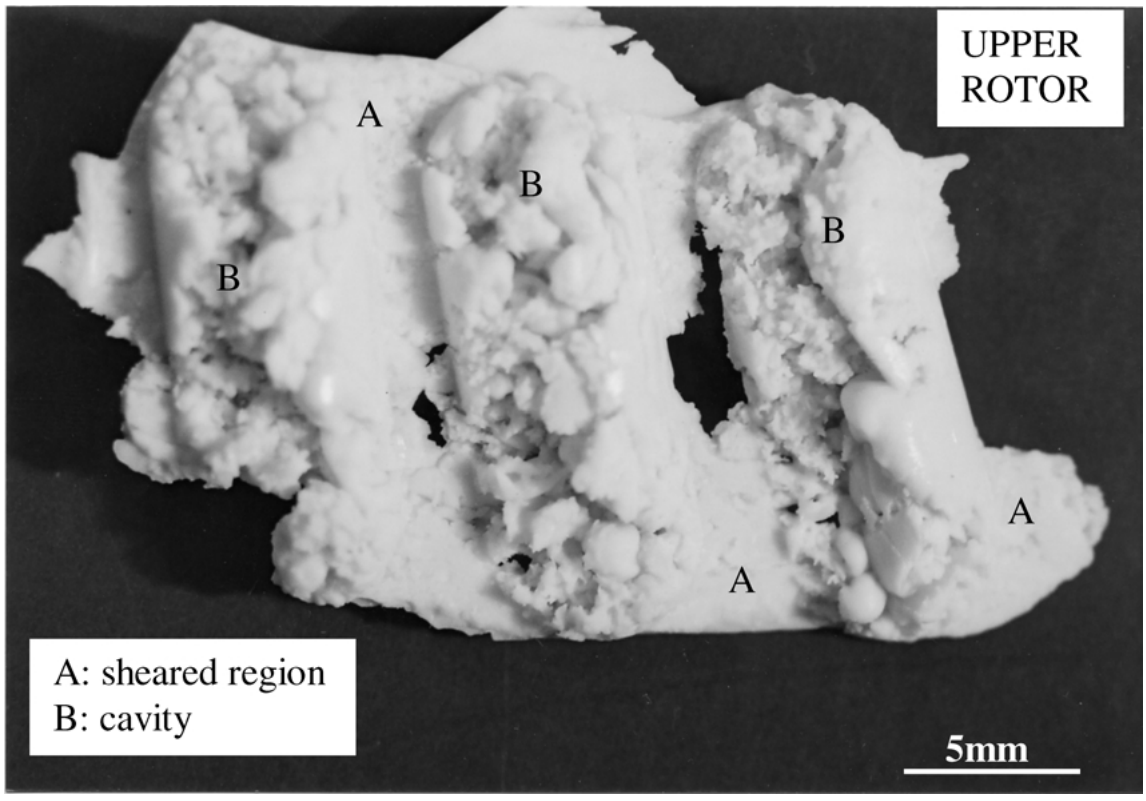

(d)

Figure 4 (*Continued*).

using scanning electron microscopy. The granules were collected from the upper rotor cavities according to the diameter of a given cavity for particle size analysis using standard sieving technique.

The concentration of the binder in the granules was determined by burning off the binder at 600°C.

3. Results

3.1. Differential scanning calorimetry (DSC)

Mettler-Toledo Model FP90 with DSC cell unit FP85 were used to evaluate the thermal characteristics of the binder (poly(ethylene glycol)) and its mixtures with the filler (calcium carbonate) over a temperature range in

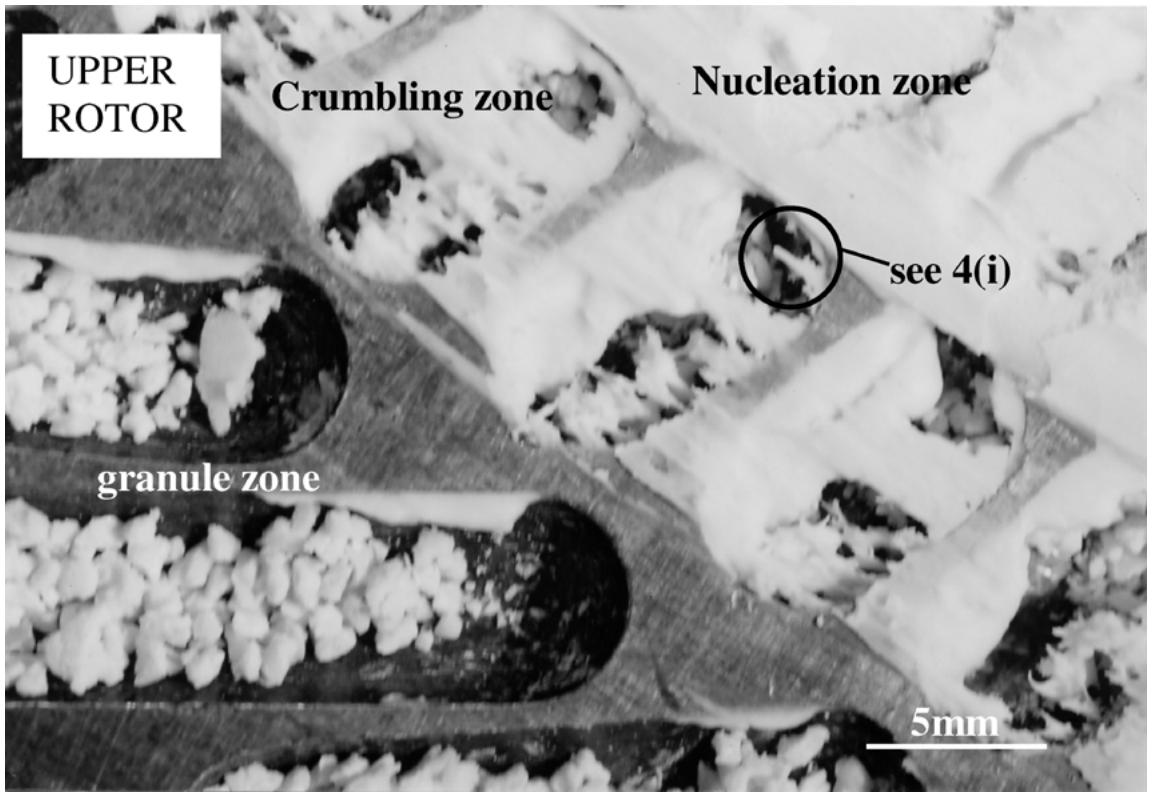

(e)

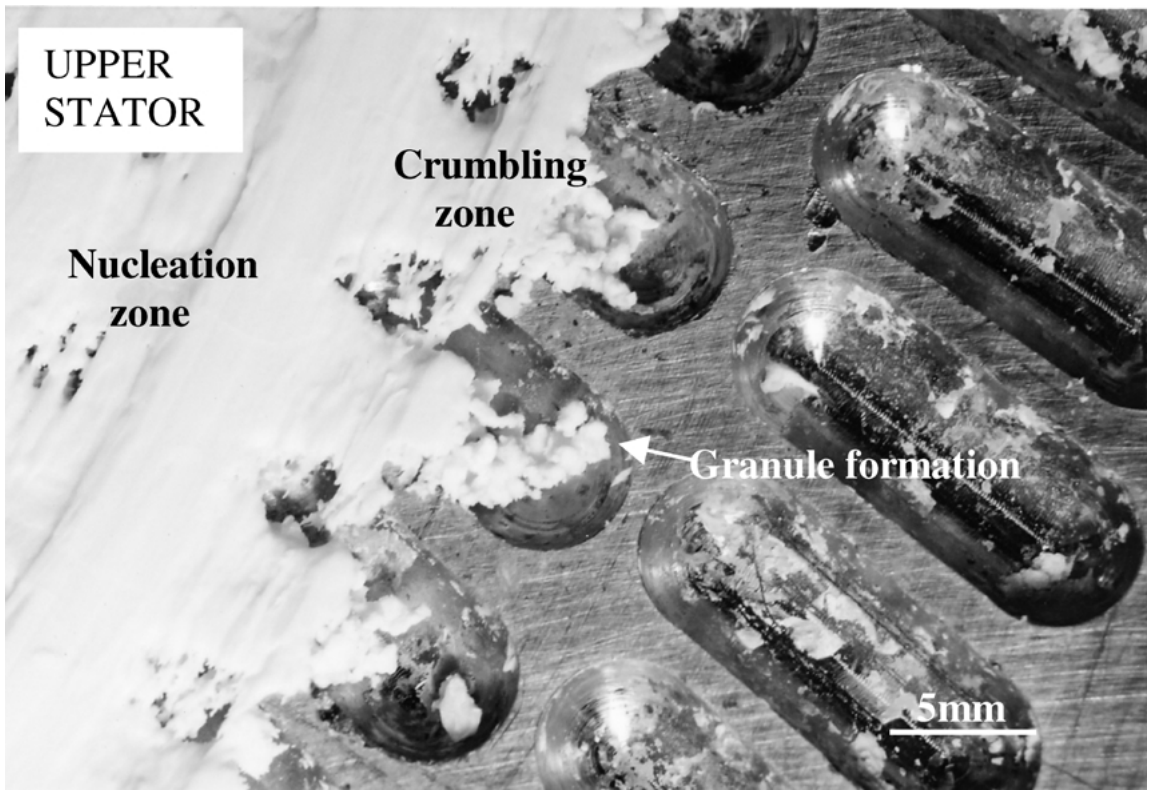

(f)

Figure 4 (*Continued*).

order to characterise the full melting and crystallisation behaviour of these materials. Both heating and cooling cycles were used. The rate of heating or cooling was 2°C/min. PEG was used as received while calcium carbonate filled PEG samples were obtained by mixing PEG and calcium carbonate in an extruder which is also used in feeding the rotating disk agglomerator/microencapsulator. Extrusion temperature was T_E = 70°C and the samples were left to solidify at room temperature.

The summary of the results is tabulated in Table I for heating and cooling cycles. PEG 10^4 is a crystalline

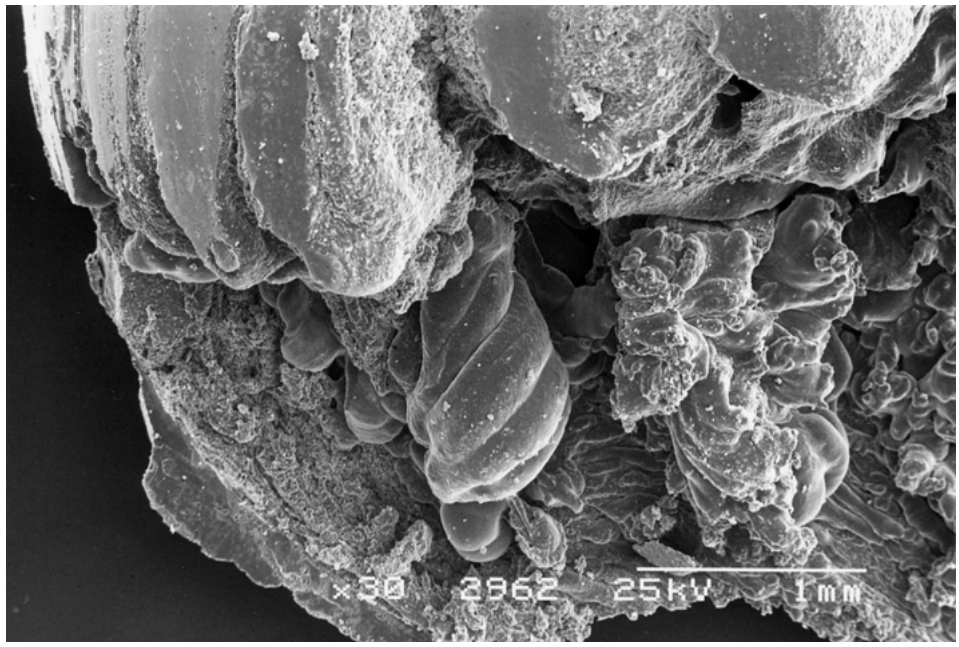

(g)

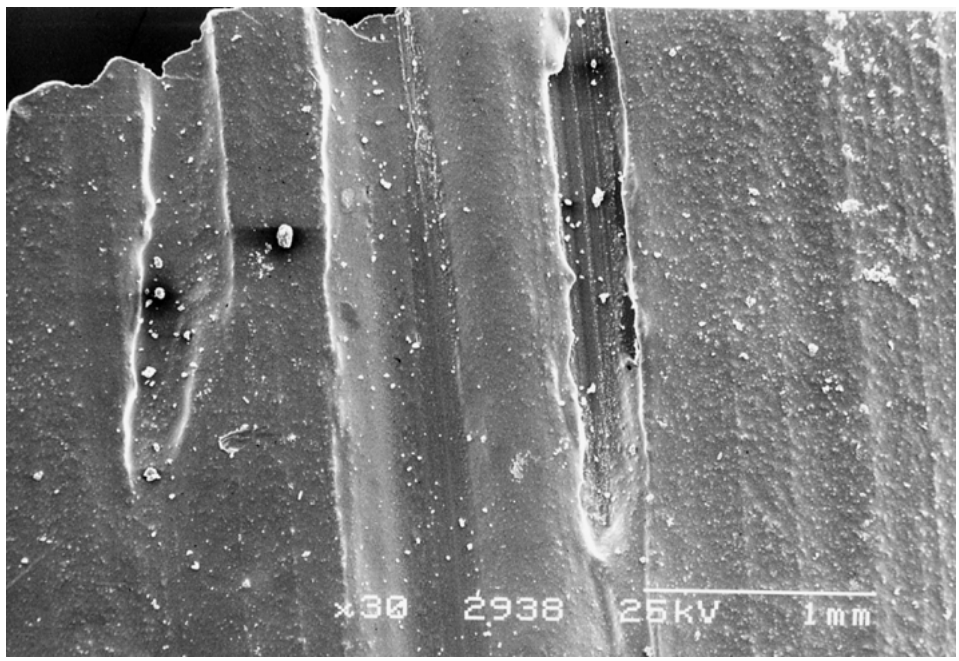

(h)

Figure 4 (*Continued*).

polymer (heat of melting $\Delta H_m = -171$ J/g and heat of crystallisation $\Delta H_c = 93$ J/g). As apparent from the reduction of the heat of crystallisation and melting, the crystallisation is greatly reduced when calcium carbonate is added. However, the presence of the filler does not appear to affect the peak melting temperature or the onset of melting ($T_m(10\%)$) or completion of melting ($T_m(95\%)$) during heating. The peak crystallisation temperature T_{cp} and the temperatures characterising the onset of crystallisation ($T_c(10\%)$) and completion of crystallisation ($T_c(95\%)$) during solidification are lowered in the presence of filler. The thermodynamic data for cooling are used in the setting of the processing temperatures (based on the peak temperatures) in the intensive granulator (i.e., upper stator temperature is 52°C, and the lower stator temperature is 45°C).

3.2. Mechanism of granulation process

Typical appearances of the upper rotor and stator surfaces after a granulation experiment are shown in Fig. 4a–f. Samples from various regions were recovered and analysed. Fig. 4a indicates that the granulation takes place over four steps. These steps are associated with the following zones. (1) Melt flow zone, with radius R_m, (2) Nucleation zone with radius R_n, (3) Crumbling (melt fracture, fragmentation) zone, with radius R_c and (4) Granule transport zone with radius $> R_c$.

In the melt flow zone, filled polymer melt follows a 3 dimensional flow path. Referred to a set of cylindrical polar coordinates (r, θ, z) located at the centre of the upper rotor, the angular motion is generated by the rotor motion, radial motion is due to the radial pressure drop and the motion in the z-direction is due to the design of

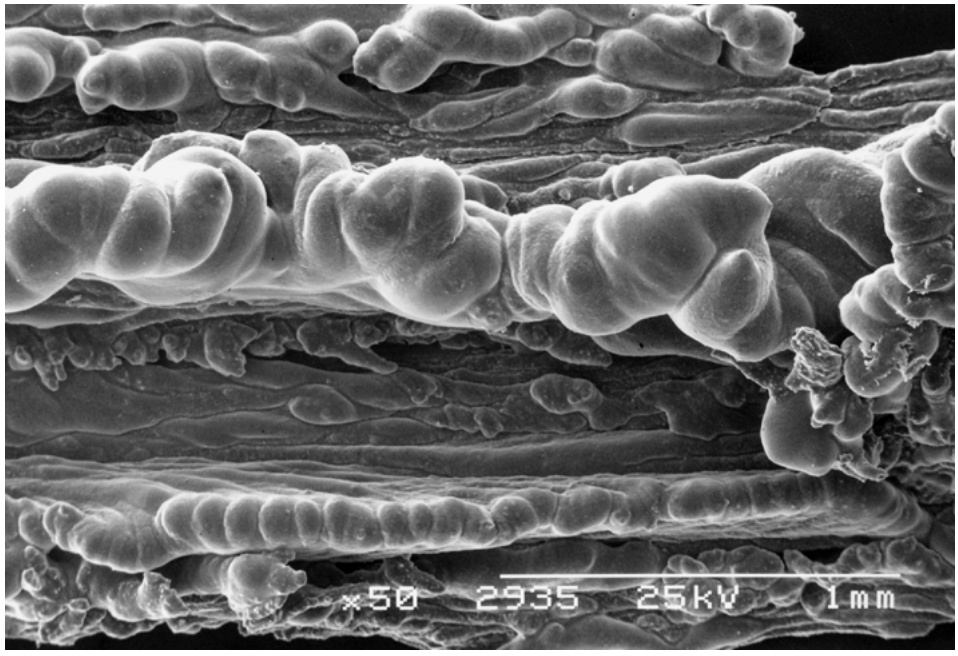

(i)

Figure 4 (*Continued*).

the cavities on the rotors and stators as well as due to the presence of the flow fields generated by the previous motions. As a result of this 3D-motion, fluid elements are transferred from cavity-to-cavity, on the rotors and stators. During this motion, polymer melt undergoes repeated cooling/heating cycles superimposed on the cooling resulting from the existence of a radial temperature gradient. Therefore, the granule nucleation takes place. It is not easy to distinguish the first two regions even though the morphology of the melt is different. In the polymer melt flow zone, solidified polymer has a smooth morphology, while in the nucleation zone, filled polymer melt has granular morphology. However, due to viscous dissipation, heat is also generated, primarily as a result of angular motion. These cooling/heating cycles result in particle solidification of the melt. Fig. 4c, d show the morphologies of a local area in the nucleation zone and they show the polymer morphology on the surface of the upper stator and upper rotor respectively. Here, the region–A is highly sheared between the rotor and stator while the region-B is the cavity into which the sheared polymer melt from region-A makes a sudden expansion. Fig. 4c, d indicate that the sheared surface is very smooth due to heat generation during shearing between rotor and stator. As can be expected, the morphology of the polymer in the upper stator (where the temperature is 52°C) is smoother than the polymer morphology on the upper rotor where the temperature is 45°C. Both the rotor and stator cavities clearly indicate the presence of agglomerate nucleation process which eventually leads to agglomeration via the fragmentation process as shown in Fig. 4e, f.

Fig. 4e illustrates the crumbling zone on the upper rotor following the nucleation zone. The crumbling zone is very short and in this particular case, crumbling takes place over the high shear rate region despite viscous heating. The appearance of the crumbling zone on the upper stator is shown in Fig. 4f which clearly illustrates the shedding of the granules from the polymer.

A closer examination (by scanning electron microscopy, SEM) of the polymer morphology in the upper rotor cavity in the nucleation zone is shown in Fig. 4g which illustrates the mixing action of the granulator as well as the presence of nucleated granules. Fig. 4h, i illustrate the morphology of the polymer in the crumbling zone as the sheared polymer enters into the cavity under the combined actions of angular and radial flow fields. The location of the sample is shown in Fig. 4e. The top surface of the polymer is smooth (Fig. 4h) while the underside of this sample shows the presence of flow instability as shown in Fig. 4i. The morphology of the polymer in this region indicates a structure very similar to that encountered in melt flow instability when there is a sudden expansion in the flow field [23, 24].

When the volume fraction of the granules reaches a certain critical value, a phase inversion takes place and the filled polymer melt crumbles, creating the granulated particles, as shown in Fig. 4a, f. Fig. 4e illustrates the appearance of the granules from the upper stator. In the present experiment, the nucleation zone occupies most of the granulator. This is due to the fact that this present processing equipment was designed as a research equipment rather than a dedicated equipment for a given product/raw-material task so that the granules are obtained within a reasonable distance from the centre of the rotors/stators. The relative radii of the zones are also dependent on the processing conditions as well the raw material characteristics.

3.3. Location of crumbling

The boundary between the crumbling and granule zones is very well defined. The distance from the centre of the upper rotor and the boundary between the crumbling

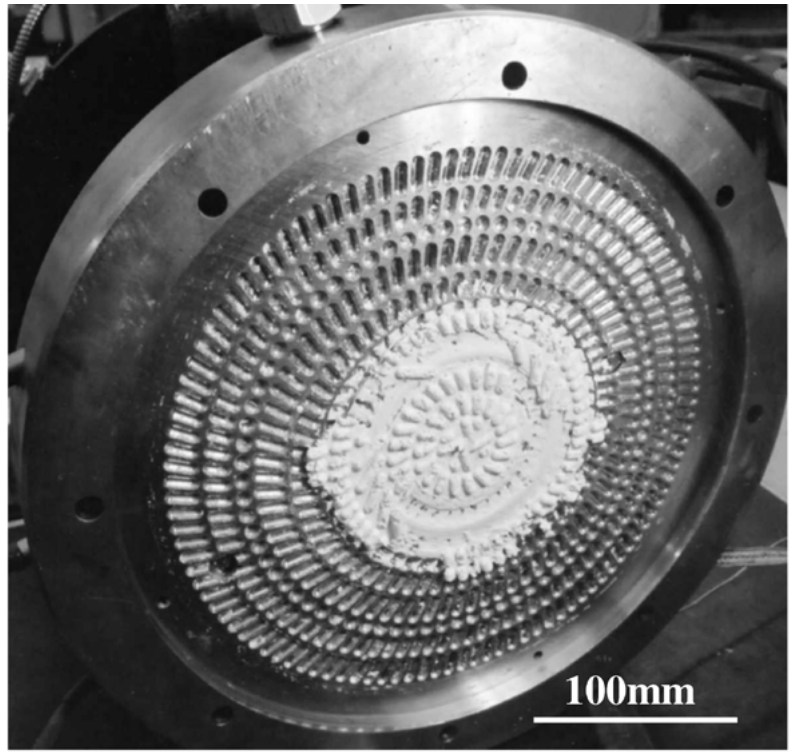

(a)

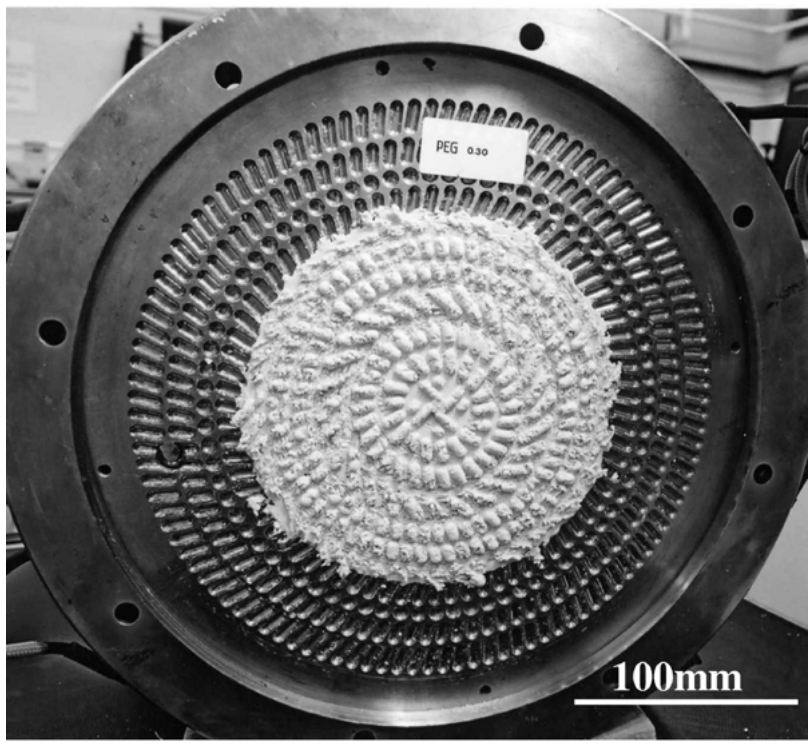

(b)

Figure 5 The effect of filler concentration on the crumbling radius as evaluated from the appearance of the upper stator. (a) PEG concentration, $C_P = 25\%$ and (b) PEG concentration, $C_P = 30\%$. The common experimental conditions were: Melt entry temperature $T_E = 70^\circ$C, upper stator temperature $T_{US} = 52^\circ$C, upper rotor temperature $T_{UR} = 45^\circ$C, lower rotor temperature $T_{LR} = 45^\circ$C and lower stator temperature $T_{LS} = 45^\circ$C. Upper rotor/stator clearance $G_U = 1.5$ mm and lower rotor/stator clearance $G_L = 0.5$ mm. Screw speed $\Omega_E = 10$ rpm, rotor speed $\Omega_R = 30$–40 rpm.

and granule zones is called the crumbling radius, R_c. This radius can be determined from the polymer imprint on the rotor or stator as shown in Fig. 4a and 5a, b. The determination of the crumbling radius R_c is very important since the size of the granulator is mainly dictated by R_c. Fig. 5 shows that if PEG concentration is 25%, $R_c = 80$ mm while for PEG concentration of 30%, $R_c = 92$ mm. The variation of R_c with the polymeric binder concentration C_P is shown in Fig. 6. They are partitioned according to the clearance G_U between upper stator and rotor. It can be seen that the crumbling radius R_c increases with increasing polymeric binder concentration since more polymer needs to be crystallised to increase the phase volume of the "solid" dispersed

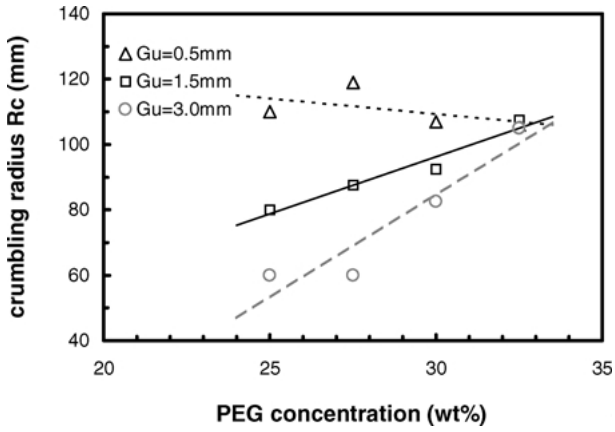

Figure 6 PEG concentration vs crumbling radius for different gaps. Processing conditions were the same as in Fig. 4 except for the upper clearance (G_U) and PEG concentration (C_P) which were changed. Amount of material processed was 300 g.

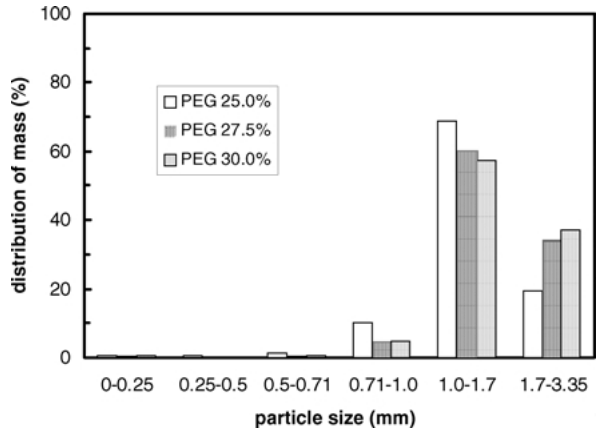

Figure 7 The effect of PEG concentration on the particle size distribution (mass basis). Processing conditions were the same as in Fig. 4 except for the upper clearance of $G_U = 1.5$ mm. In all cases, samples were collected from the cavity ring 10. Amount of material processed was 300 g.

phase to cause crumbling. Therefore, the polymer/filler melt residence time has to be increased. Furthermore, if the polymer concentration is low, the fraction of polymer immobilised by the filler will also be high.

When the rotor/stator gap is small, more viscous heat is generated and the flow rate through the granulator is high and consequently, the crumbling radius should increase. However, at a constant heat removal rate from the melt, a smaller amount of filled polymer melt needs to be cooled when the gap G_U is small. Thus we should expect a smaller crumbling radius. Therefore, these two effects oppose each other. As seen from Fig. 6, the crumbling radius increases with increasing polymer concentration. The reduction in rotor-stator clearance also increases the crumbling radius in general.

3.4. The effect of binder concentration on granule size distribution characteristics

The transient particle size characteristics of the granules are determined by measuring the particle size distribution from where average particle size at 50% cumulative $D(50)$ and particle size span, S are evaluated. These granule characteristics are dependent on the processing conditions as well as on the composition of the filler/polymer system. The effect of the various parameters on the granule particle size characteristics are evaluated below.

After the granulation experiments, the granules in the cavities at a given radius are collected and their size distribution is analysed. Fig. 7 shows the distribution of mass fraction versus particle size as a function of binder concentration. The corresponding cumulative % versus particle size is shown in Fig. 8. During the transport of the granules, larger particles move faster and therefore the particle size analysis at each ring of cavities yield higher mean granule size as newly generated particles are transported radially outward. This is illustrated in Fig. 9 where the variation of particle size at 50 percentile $D(50)$ is shown as a function of cavity ring number.

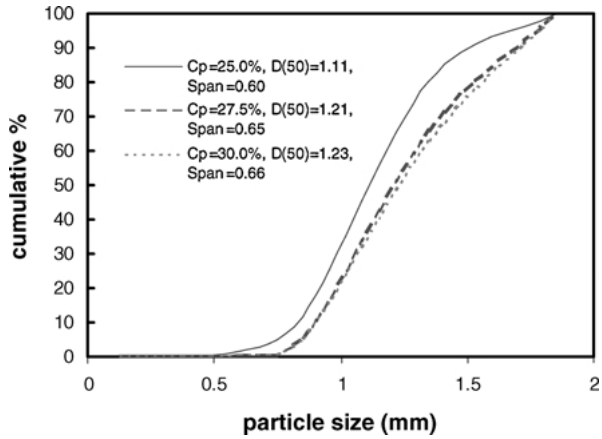

Figure 8 Variation of the particle size distribution (mass basis) with different PEG concentrations. The concentrations were selected $C_P = 25\%$, $C_P = 27.5\%$ and $C_P = 30\%$, and $G_U = 1.5$ mm. The samples were collected from the same location on the rotor i.e., the cavity ring 10, at which the mean radius was 128 mm from the centre. The $D(50)$ value and span are shown in the profiles. Processing conditions were as in Fig. 7.

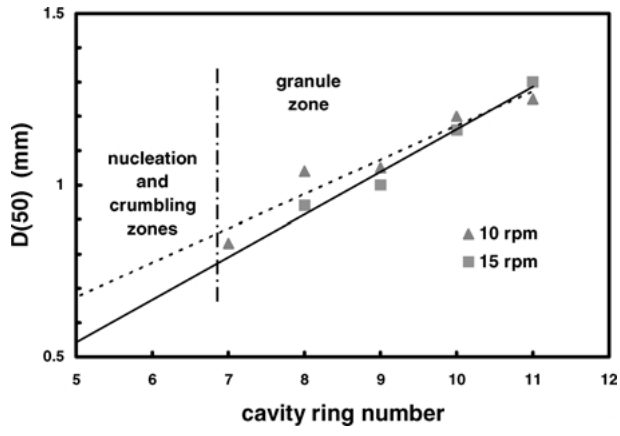

Figure 9 Variation of average granule size, $D(50)$ with cavity ring number at two different extruder speeds. PEG concentration, $C_P = 25\%$, upper rotor/stator gap $G_U = 1.5$ mm. Other processing conditions were identical to those in Fig. 7.

3.5. The effect of melt flow rate on particle size distribution

Fig. 9 also illustrates the dependence of the average granule size $D(50)$ on the speed of the extruder. The polymer/filler melt flow rate into the extruder is controlled through the extruder screw speed (Ω_E). Most of the experiments were carried out at extruder screw speed of $\Omega_E = 10$ rpm which corresponds to the melt flow rate of 10 g/min (with 25% PEG). Due to the heat transfer rate limitations of the current design of the granulator, and the extruder size, the range of the melt flow rate was rather narrow within 10 rpm–15 rpm. Within this limited flow rate range the effect of melt flow rate on the particle size development is not very significant as observed in Fig. 9, which shows the $D(50)$ vs cavity ring number. Fig. 9 also illustrates the location of the crumbling radius when $\Omega_E = 10$ rpm. Both the average granule size and size span (data not shown in the figure) are not significantly affected by the extrusion speed. Similar to our previous examples [12], average granule size $D(50)$ increases with increasing cavity number while the particle size span decreases and finally approaches to a plateau.

3.6. Addition of TiO_2 powder

Fig. 10 shows the general view of the rotor surface after a granulation experiment. In the experiment, using an auger feeder, TiO_2 powder was added into the filled polymer melt immediately after phase inversion during the granulation through the auger. The extra powder helped the solidification and is useful to increase the particle content of the agglomerates. The granule sample was studied by SEM. It was found that TiO_2 powder only coated the surface of the granules thus forming a core-shell particle structure.

4. Discussion

A novel granulation technique and an equipment to achieve it are described above. The technique is based on the non-isothermal flow induced phase inversion technique in which the transformation from a highly viscous fluid state (paste) to particulate state (granules) is achieved through a thermo-mechanical fracture process. The equipment for the process consists essentially of rotor and stator disks containing cavities, the design of which results in a 3 dimensional flow path of the polymer/filler melt as well as the granules. During the non-isothermal polymer/filler melt flow, fluid also undergoes repeated extensional and shear flows, similar to that observed in the so called Multiple Expansion—Contraction Static Mixer [10, 11].

The polymer melt enters into the gap between the rotor and stator at 70°C. The temperature of the stator was 52°C which is close to the PEG solidification temperature, while the rotor temperature is 45°C which is close to the temperature when 90% of PEG solidifies. As the polymer/filler melt flows radially outwards with a 3D—flow path, it also cools down thus increasing its viscosity. Fractional solidification, coupled with such flow phenomena, as flow induced phase inversion and flow induced polymer crystallisation [8–11, 24], the fraction of solid dispersed phase increased. The presence of granules dispersed into the polymer melt was observed through optical and scanning electron microscopy in the granule nucleation zone.

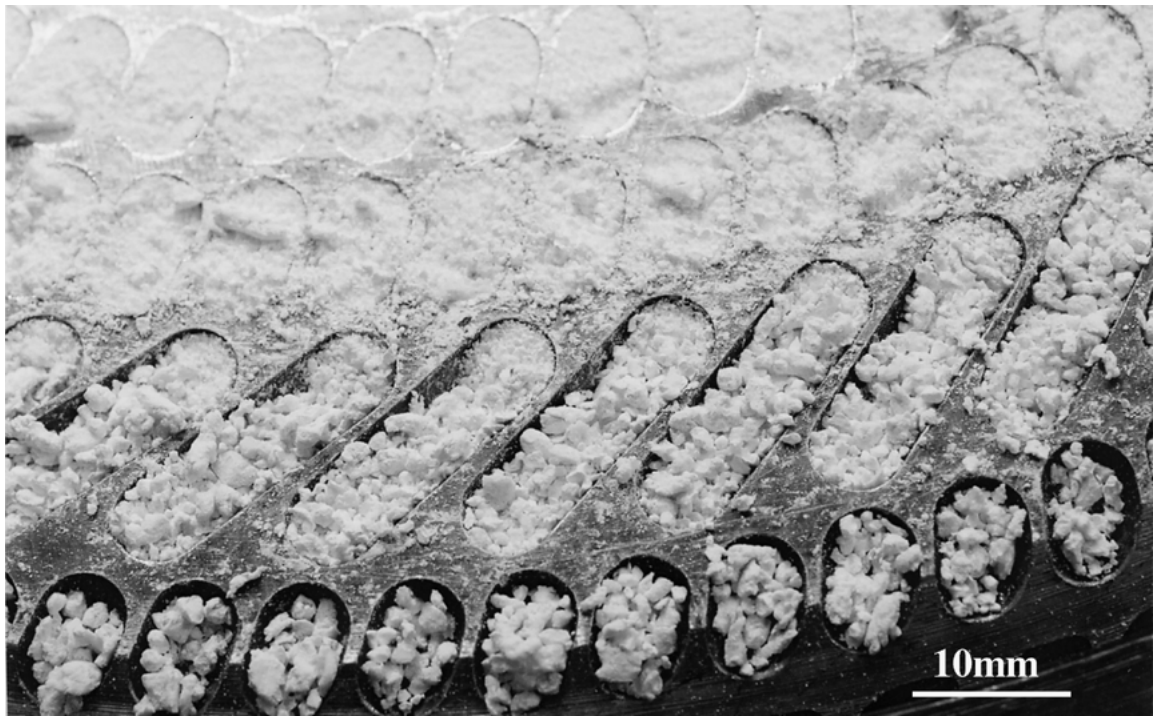

Figure 10 The general view of the upper rotor after adding TiO_2 particles at a location just after the formation of the granules (after crumbling). Experimental conditions were the same as in Fig. 6 when PEG concentration, $C_P = 27.5\%$ (TiO_2 free basis), $G_U = 1.5$ mm. The rate of addition of TiO_2 was 2 g/min. Extruder speed was 10 rpm, rotor speed 30–45 rpm, 27 g TiO_2 was added.

When the phase volume of the solid dispersed phase exceeds ca. 74%, a phase transformation takes place and particle-in-polymer melt is converted into granules. This transformation takes place almost instantaneously over a short distance, described as the 'crumbling zone' with radius R_c. The determination of the crumbling radius is important since it dictates the size of the equipment.

It is possible to reduce the 'crumbling radius' by more effective heat transfer as well as by using high filler concentration. This can be achieved by adding a 'crumbling agent' in the nucleation zone. Addition of colloidal particles into the melt accelerates crumbling as discussed previously [5–9]. Another important purpose of crumbling agent is the modification of the surface characteristics of the newly formed granules.

Any measure to increase the effective dispersed phase volume of the polymer/filler system will result in reduced crumbling radius. In the absence of additional crumbling agent, the most important processing parameter affecting crumbling radius is the reduction in melt temperature. If the internal heat generation due to viscous heating is high, crumbling is also delayed. Therefore, small rotor—stator clearance will result in a large crumbling radius.

After crumbling, granules are transported radially outward through a 3D flow path while undergoing cooling. This zone is described as granule zone. In this zone, granules undergo insignificant degree of attrition since the rotor—stator cavity arrangement allows the transport of the granules through cavity hopping. However, the addition of the crumbling agent in the crumbling zone results in comminution and surface coating of the granule particles. If no crumbling agent is added after crumbling, granule size increases as the granules flow radially outwards. However this is a transient effect due to particle segregation.

5. Conclusions

The mechanism of granulation in a novel intensified granulator was evaluated through SEM and visualisation of the polymer at various locations in the granulator. It is shown that, due to the presence of cavities in the rotor and stator disks and the imposition of a temperature gradient across the disks, granulation starts as a nucleation process and the transformation from a melt state to a granule state occurs almost instantaneously in which the granule particles are shed from the melt. This technique produces granules with a narrow size distribution and constant filler concentration independent of granule size. Average granule size is similar to the size of the rotor—stator clearance. Granules with a surface coating can also be obtained by using colloidal crumbling agent introduced into the granulator at the crumbling zone.

Acknowledgements

We are grateful to Dr. Robert Addleman (Rosand Precision Ltd.) for many helpful discussions and the construction of the intensified ITIG granulator. This research was supported by the Engineering and Physical Sciences Research Council (EPSRC) of the UK, AstraZeneca, Carl Stewart Ltd., Syngenta, Rosand Precision Ltd. and Thermo Haake. Their support is gratefully acknowledged.

References

1. D. S. T. HSIEH, in "Controlled Release Systems: Fabrication Technology" (CRC Press, Boca Raton, 1988) Vol. 2.
2. C. E. CAPES, in "Handbook of Powder Technology," edited by J. C. Williams and T. Allen (Elsevier, Amsterdam, 1980) Vol. 1.
3. W. PIETSCH, *Chem. Eng. Prog.* **92**(4) (1996) 29.
4. F. HOORNAERT, P. A. L. WAUTERS, G. M. H. MEESTERS, S. E. PRATSINIS and B. SCARLETT, *Powder Technology* **96** (1998) 116.
5. G. AKAY, *Polym. Eng. Sci.* **34** (1994) 865.
6. *Idem.*, Agglomerated Abrasive Material, US Patent no. 4 988 369 (1991) European Patent no. 307278 (1992) and Japanese Patent no. 940 37634 (1994).
7. *Idem.*, in "Polymer Powder Technology," edited by M. Narkis and N. Rosenzweig (Wiley, New York, 1998) p. 542.
8. *Idem.*, Coating Process, European Patent no. 382 464 (1992), Australian Patent no. 633 299 (1993).
9. *Idem.*, *Polym. Eng. Sci.* **30** (1990) 1361.
10. *Idem.*, *Chem. Eng. Sci.* **53** (1998) 203.
11. *Idem.*, European Patent no. 649 867 (2002).
12. G. AKAY and L. TONG, *Ind. Eng. Chem. Res.* **41** (2002) 5436.
13. L. TONG and G. AKAY, *J. Mater. Sci.* **37** (2002) 4985.
14. G. AKAY and L. TONG, *J. Colloid Interface Sci.* **239** (2001) 342.
15. G. AKAY, L. TONG, M. HOUNSLOW and A. S. BURBIDGE, *Colloid and Polymer Sci.* **279** (2001) 279.
16. G. AKAY and L. TONG, *J. Mater. Sci.* **35** (2000) 3699.
17. G. AKAY, L. TONG, H. BAKR, R. A. CHOUDHERY, K. MURRAY and J. WATKINS, *ibid.* **37** (2002) 4811.
18. G. AKAY, in "Recent Advances in Transport Phenomena," edited by I. Dincer and M. F. Yardim (Elsevier, Paris, 2001) p. 11.
19. A. CASALE and R. S. PORTER, in "Polymer Stress Reactions" (Academic Press, New York, 1978) Vol. 1.
20. G. AKAY, *Polym. Eng. Sci.* **22** (1982) 798.
21. I. SEKIGUCHI, in "Process in Powder Technology Handbook," edited by K. Gotoh, H. Masuda and K. Higashitani (Marcel Dekker Inc., New York, 1997) Vol. 7.
22. G. AKAY and L. TONG, in "Progress in Transport Phenomena," edited by S. Dost, H. Struchtrup and I. Dincer (Elsevier, Paris, 2002) p. 681.
23. G. AKAY, V. J. PRICE and S. Y. CHAN, Flow Induced Phase Inversion in the Intensive Agglomeration/Microencapsulation of Powders, in Recent Advances in Particle Technology, IChemE CD-Rom, 1998.
24. G. AKAY, in "Encyclopaedia of Fluid Mechanics," edited by N. P. Cheremisinoff (Gulf Publishing, Houston, 1986) Vol. 1, p. 1155.

Received 31 January
and accepted 30 April 2003